**BICC1 Interacts with PKD1 and PKD2 to Drive Cystogenesis in ADPKD**

Uyen Tran[1*], Andrew J Streets[2*], Devon Smith[2*], Eva Decker[3], Annemarie Kirschfink[4], Lahoucine Izem[1], Jessie M. Hassey[1], Briana Rutland[1], Manoj K Valluru[2], Jan Hinrich Bräsen[5], Elisabeth Ott[6], Daniel Epting[6], Tobias Eisenberger[3], Albert CM Ong[2†], Carsten Bergmann[3,6†], Oliver Wessely[1†]

[1]Department of Cardiovascular & Metabolic Sciences, Lerner Research Institute, Cleveland Clinic Foundation, Cleveland, USA

[2] Kidney Genetics Group, Division of Clinical Medicine, School of Medicine and Population Health, University of Sheffield, Beech Hill Road, Sheffield S10 2RX, United Kingdom

[3]Medizinische Genetik Mainz, Limbach Genetics, Mainz, Germany

[4]Department of Human Genetics, RWTH University, Germany

[5]Institute of Pathology, Medizinische Hochschule Hannover, Germany

[6]Department of Medicine IV, Faculty of Medicine, Medical Center-University of Freiburg, Germany

*Equal contribution

[†]Co-corresponding authors

Correspondence:

Oliver Wessely (wesselo@ccf.org), Carsten Bergmann (carsten.bergmann@medgen-mainz.de) and Albert Ong (a.ong@sheffield.ac.uk)

Running title: *BICC1-Polycystin Interaction in ADPKD*

Word Count (excluding references): 4,252

**ABSTRACT**

Background: Autosomal dominant polycystic kidney disease (ADPKD) is primarily of adult-onset and caused by pathogenic variants in *PKD1* or *PKD2*. Yet, disease expression is highly variable and includes very early-onset PKD presentations *in utero* or infancy. In animal models, the RNA-binding molecule Bicc1 has been shown to play a crucial role in the pathogenesis of PKD.

Methods: To study the interaction between *BICC1, PKD1 and PKD2* we combined biochemical approaches, knockout studies in mice and *Xenopus,* genetic engineered human kidney cells as well as genetic association studies in a large ADPKD cohort.

Results: We first demonstrated that BICC1 physically binds to the proteins Polycystin-1 and -2 encoded by *PKD1* and *PKD2* via distinct protein domains. Furthermore, PKD was aggravated in loss-of-function studies in *Xenopus* and mouse models resulting in more severe disease when *Bicc1* was depleted in conjunction with *Pkd1 or Pkd2*. Finally, in a large human patient cohort, we identified a sibling pair with a homozygous *BICC1* variant and patients with very early onset PKD (VEO-PKD) that exhibited compound heterozygosity of *BICC1* in conjunction *with PKD1 and PKD2* variants. Genome editing demonstrated that these *BICC1* variants were hypomorphic in nature and impacted disease-relevant signaling pathways.

Conclusions: These findings support the hypothesis that *BICC1* cooperates functionally with *PKD1 and PKD2*, and that *BICC1* variants may aggravate disease severity highlighting RNA metabolism as an important new concept for disease modification in ADPKD.

## INTRODUCTION

Autosomal dominant polycystic kidney disease (ADPKD) is the most frequent life-threatening genetic disease and one of the most common Mendelian human disorders with an estimated prevalence of 1/400-1000.[1,2] This equates to around 12.5 million affected individuals worldwide. About 5-10% of all patients requiring renal replacement therapy are affected by ADPKD. The majority of ADPKD patients carry a pathogenic germline variant in the *PKD1* or *PKD2* gene and present with the disease in adulthood.[2-4] However, occasionally, ADPKD can manifest in infancy or early childhood (< 2 years, very-early onset ADPKD (VEO-ADPKD)), and in late childhood or early teenage years (2-16 years, early-onset ADPKD (EO-ADPKD)).[5,6] VEO patients and fetuses often present with a Potter sequence and significant peri- or neonatal demise, which can be clinically indistinguishable from a typical Autosomal Recessive Polycystic Kidney Disease (ARPKD) presentation caused by *PKHD1* mutations.[7,8] However, in contrast to VEO/EO-ADPKD, ARPKD kidneys invariably manifest as fusiform dilations of renal collecting ducts and distal tubules that usually remain in contact with the urinary system.[4] Co-inheritance of an inactivating *PKD1* or *PKD2* mutation with an incompletely penetrant minor PKD allele with *in trans* provides a likely explanation for VEO-ADPKD.[9] In fact, we recently reported that the majority (70%) of VEO-ADPKD cases in an international diagnostic cohort had biallelic *PKD1* variants (i.e., a pathogenic variant *in trans* with a hypomorphic, low penetrance variant), while cases of biallelic *PKD2* and digenic *PKD1/PKD2* were rather rare.[10] In line with the dosage theory for PKD,[11] several other genes (*GANAB, DNAJB11, ALG8, ALG9, IFT140*) have been associated with a dominant, but late-onset atypical adult presentation and sometimes incomplete penetrance.[4,12-15] Yet, not all VEO/EO-ADPKD patients can be explained by monogenic inheritance suggesting digenic or oligogenic inheritance causes.

Previous data from mouse, *Xenopus* and zebrafish suggest a crucial role for the RNA-binding protein Bicc1 in the pathogenesis of PKD, although *BICC1* mutations in human PKD have not been previously reported.[16-22] BICC1 encodes an evolutionarily conserved protein that is characterized by up to five N-terminal KH/KH-like RNA-binding domains and a C-terminal SAM domain.[23-26] The protein localizes to

cytoplasmic foci involved in RNA metabolism and has been shown to regulate the expression of several genes such as *Pkd2, Adcyd6* and *Pkia* in the kidney.[22,27] We now present data providing a mechanistic model linking BICC1 with the three major cystic proteins. We show that BICC1 physically interacts with the PKD1 (PC1) and the PKD2 (PC2) protein in human kidney cells. We also demonstrate that *Pkd1* and *Pkd2* modifies the cystic phenotype in *Bicc1* mice in a dose-dependent manner and that Bicc1 functionally interacts with Pkd1, Pkd2 and Pkhd1 in the pronephros of *Xenopus* embryos. Finally, this interaction is supported by human patient data where *Bicc1* alone or in conjunction with *PKD1* or *PKD2* is involved in VEO-PKD.

## METHODS

### Cell Culture and Biochemical Studies

The characterization of the interaction between BICC1, PC1 and PC2 as well as the analysis of the human BICC1 variants were performed using standard approaches detailed in the Supplementary Methods.

### Animal Studies

Mouse and *Xenopus laevis* studies were approved by the Institutional Animal Care and Use Committee at the Cleveland Clinic Foundation and LSU Health Sciences Center (present and former employer of Dr. Wessely) and adhered to the National Institutes of Health Guide for the Care and Use of Laboratory Animals. Experimental design and data interpretation followed the ARRIVE1 reporting guidelines.[28]

### International Diagnostic Clinical Cohort

Research was performed following written informed consent and according to the declaration of Helsinki and oversight was provided by the Medizinische Genetik Mainz. DNA extraction was performed according to standard procedures (see Supplementary Methods for details).

### Statistical analysis

Data are presented as mean values ± SEM. Paired and unpaired two-sided Student’s t test was used for

statistical analyses with a $P < 0.05$ indicating statistical significance. Measurements were taken from distinct biological samples. Analyses were carried out using Prism 10 (Graphpad).

## RESULTS

### Bicc1 Interacts with PC1 and PC2

Loss of Pkd1 has been associated with lower expression of Bicc1.[29] Furthermore, Bicc1 has been shown to regulate *Pkd2* expression in cellular and animal models.[22,30,31] However, whether this is due to direct protein-protein interactions between BICC1, PKD1 (PC1) and PKD2 protein (PC2) have not been investigated. In pilot experiments, BICC1 was detected by mass spectrometry in a pulldown assay from cells stably expressing a Polycystin-1 PLAT domain (Polycystin-1, Lipoxygenase, Alpha-Toxin)-YFP fusion.[32] The direct binding between the PC1-PLAT domain and Bicc1 was confirmed using *in vitro* binding assays, but also detected binding to the PC1 C-terminus (CT1) (**Supplementary Fig. S2a,c**).

Utilizing recombinant GST domains of PC1 and PC2, we demonstrated that BICC1 binds to both proteins in GST-pulldown assays (**Fig. 1a, b**). In the case of PC1, myc-mBICC1 strongly interacted with its C-terminus but its interaction was significantly reduced by a PC1-R4227X truncation mutation (**Fig. 1b**). In the case of PC2, myc-mBICC1 associated with both recombinant GST N-terminal and C-terminal fusions. To investigate whether binding was direct or indirect, we performed *in vitro* binding assays using *in vitro* translated myc-Bicc1 and recombinant PC1 and PC2 domains (**Fig. 1c**). GST-pulldowns confirmed a direct interaction between myc-Bicc1 and the C-terminus of PC1 but not a PC1-R4227X mutant (**Fig. 1d** and **Supplementary Fig. S2d**). Similarly, myc-Bicc1 interacted directly with the PC2 N-terminus. While binding was stronger with the distal sequence (NT2 aa101-223) both N-terminal fragments contributed to the overall binding to Bicc1 (**Fig. 1d**). Interestingly, no direct interaction between Bicc1 and the PC2 C-terminus was detected (**Supplementary Fig. S2b,c**) suggesting that the observed *in vivo* interaction with Bicc1 is indirect. Finally, immunoprecipitation using lysates from human kidney

epithelial cells (UCL93) to assay endogenous, non-overexpressed proteins showed that PC1, PC2 and BICC1 form protein complexes *in vivo* (**Fig. 1e,f**).

**Binding of Bicc1 to the Polycystins Requires Different Interaction Motifs**

To define the PC1/PC2 interaction domain(s) in Bicc1, we generated deletion constructs lacking the SAM domain (myc-mBicc1-ΔSAM) or the KH domains (myc-mBicc1-ΔKH) (**Fig. 2a**) and studied them by co-IP. Full-length PC1 co-immunoprecipitated with full-length myc-mBicc1 (**Fig. 2b,c**). Deleting the SAM domain reduced the association to PC1 by ~55% compared to full-length myc-mBicc1. Surprisingly, an 8-fold stronger interaction was observed between full-length PC1 and myc-mBicc1-ΔKH compared to myc-mBicc1 or myc-mBicc1-ΔSAM. These results suggest that the interaction between PC1 and Bicc1 requires the SAM but not the KH domains (or the first 132 amino acids of Bicc1). It also suggests that the N-terminus could have an inhibitory effect on PC1-BICC1 association.

Similar experiments were performed to define the Bicc1 interacting domains for PC2 (**Fig. 2d,e**). Full-length PC2 (PC2-HA) interacted with full-length myc-mBICC1. However, unlike PC1, PC2 interacted with myc-mBICC1-ΔSAM, but not myc-mBICC1-ΔKH suggesting that PC2 binding is dependent on the N-terminal domains but not the SAM domain.

**Cooperativity of Bicc1 with other PKD genes**

Since our biochemical analysis indicated a direct interaction between BICC1, PC1 and PC2, we wondered whether this is biologically relevant. If this were the case, BICC1 should cooperate with other PKD genes and reducing BICC1 activity in conjunction with reducing either PKD1 or PKD2 activity should still cause a cystic phenotype. We first addressed this question in the *Xenopus* system (**Fig. 3**), where we previously reported that knockdown of Bicc1 or Pkd2 using antisense morpholino oligomers (MOs) causes a PKD phenotype.[21,22] This phenotype is characterized by the formation of edema due to impaired kidney function, dilated tubules and the loss of *Nbc1* mRNA expression in the late distal tubule of the kidney (**Fig. 3e-g”**). An identical phenotype was observed when we targeted Pkd1 and Pkhd1

using splice site MOs (*Pkd1-sMO* or *Pkhd1-sMO*, **Fig. 3h-i"**). To test whether combined knockdowns cause a similar phenotype, we titrated each of the four MOs to a concentration that on its own resulted in little phenotypic changes upon injection into *Xenopus* embryos (**Fig. 3j,k** and **Supplementary Figure S1c**). However, combining *Bicc1-MO1+2* with *Pkd1-sMO*, *Pkd2-MO* or *Pkhd1-sMO* at suboptimal concentrations resulted in a strong PKD phenotype. While injections with individual MOs developed edema in about 10% of the embryos, co-injections caused edema formation in almost 100% of the embryos (**Fig. 3j**, last 3 columns). A similar result was seen for the expression of *Nbc1* in the late distal tubule (**Fig. 3k**). Single MO injections showed some changes in gene expression, but double MO injections had a highly synergistic effect resulting in a near complete loss of *Nbc1*. Together, these data demonstrate that lowering Bicc1 activity sensitizes the *Xenopus* embryos to changes in the expression of other PKD genes. Finally we expanded our analysis to *Pkhd1*, the gene mutated in ARPKD.[33] Like *Bicc1*, *Pkd1* and *Pkd2*,[21,34,35] *Pkhd1* was also expressed in the pronephric kidney, displayed a PKD phenotype upon knockdown using a splice site MO (*Pkhd1-sMO*) and cooperated with Bicc1 when analyzed at suboptimal MO concentrations (**Fig. 3j,k**).

We next investigated the interactions in mice focusing on the hypothesis that removal of *Bicc1* and *Pkd2* results in an aggravated kidney phenotype. Both *Bicc1* and *Pkd2* mutant mice develop cystic kidneys as early as E15.5.[22,36] As this is the earliest time point cystic kidneys can be observed, crossing those strains did not allow us to assess cooperativity (data not shown). Moreover, like in the case of compound *Pkd1/Pkd2* mutants,[37] kidneys from $Bicc1^{+/-}$:$Pkd2^{+/-}$ did not exhibit cysts (data not shown). Thus, we instead used mice carrying the Bicc1 hypomorphic allele *Bpk*, which develop a cystic kidney phenotype postnatally.[18,38] To assess cooperativity, we removed one copy of *Pkd2*. Comparing the kidneys of $Bicc1^{Bpk/Bpk}$:$Pkd2^{+/-}$ to those of $Bicc1^{Bpk/Bpk}$:$Pkd2^{+/+}$ at postnatal day P14 revealed that the compound mutant kidneys were larger and more translucent (**Fig. 4a**). Moreover, total kidney weight (KW) and kidney/body weight ratios (KW/BW) were significantly different (**Fig. 4b,d**). Interestingly, the

reduction in *Pkd2* gene dose affected the progression of the disease, but not its onset. Performing the same analysis at postnatal day P4 did not show any differences (**Fig. 4c**).

Next, we performed a similar mouse study for *Pkd1* by reducing the gene dose of *Pkd1* postnatally in the collecting ducts using a *Pkhd1-Cre* as previously described[39] (in the following referred to as $Pkd1^{CD-}$). Similar to the *Bicc1/Pkd2* scenario, $Bicc1^{Bpk/Bpk}$:$Pkd1^{+/CD-}$ appeared larger when comparing kidneys from littermates (**Fig. 4e**). Yet, aggregating the data from all $Bicc1^{Bpk/Bpk}$:$Pkd1^{+/+}$ and $Bicc1^{Bpk/Bpk}$:$Pkd1^{+/CD-}$ mice did not show differences in total KW and KW/BW ratios (data not shown and **Supplementary Fig. S3c**). Only, when restricting the analysis to littermates, did we detect a statistically significant difference in KW/BW ratio (**Fig. 4f**). To further corroborate this, we determined the cystic index for proximal tubules and collecting ducts using LTA and DBA staining, respectively. This showed an increase in collecting duct cysts upon removal of one copy of *Pkd1* (**Fig. 4h**). Like in the case of *Pkd2*, the phenotype seems to be correlated with cyst expansion and not the onset, as there was no difference at postnatal day P7 (**Fig. 4g**). It is noteworthy that neither the *Bicc1/Pkd2* nor the *Bicc1/Pkd1* compound mutants showed an aggravated kidney function based on Blood Urea Nitrogen (BUN) levels (**Supplementary Fig. S3a,b,d**) likely due to the aggressive nature of the $Bicc1^{Bpk/Bpk}$ phenotype. Moreover, like in the case of compound heterozygous *Pkd1/Pkd2* mutants, compound heterozygous *Bicc1/Pkd2* nor the *Bicc1/Pkd1* did not result in a detectable kidney phenotype (**Fig. 4b-d** and **Supplementary Fig. S3a,c,d**). Together these data demonstrate that BICC1 cooperates with the major PKD genes, *PKD1* and *PKD2*, and that compound situations aggravate the Bicc1 cystic kidney phenotype.

Finally, to better understand how Bicc1 would exert such a phenotype, we analyzed the expression of the PKD genes in the $Bicc1^{Bpk/Bpk}$ mice. We have previously demonstrated that *Pkd2* levels are reduced in a complete Bicc1 null mice,[22] performing qRT-PCR of P4 kidneys (i.e. before the onset of a strong cystic phenotype), revealed that *Pkd1*, *Pkd2* and *Pkhd1* were statistically significantly down-regulated (**Fig. 4i**). This was confirmed by protein analysis for PC2 (**Fig. 4j** and **Supplementary Fig.**

**S3e**). Together, these data support a model, in which Bicc1 acts as a positive regulator of PKD gene expression. In the presence of 'sufficient' amounts of PC1/PC2 complex, it is tethered to the complex and remains biologically inactive (**Fig. 4k**). However, once the levels of the PC1/PC2 complex are reduced, Bicc1 is now present in the cytoplasm to promote expression of the PKD proteins, thereby raising their levels (**Fig. 4l**), which then in turn will 'shutdown' Bicc1 activity by again tethering it to the plasma membrane.

### ***BICC1* Variants in Patients with early and severe Polycystic Kidney Disease**

To evaluate whether these interactions are relevant for human PKD, we analyzed an international cohort of 2,914 PKD patients by massive parallel sequencing (MPS) [40,41] focusing on VEO-ADPKD patients with the hypothesis that *BICC1* variants may lead to a more severe and earlier PKD phenotype. While variants in *BICC1* are very rare, we could identify two patients with *BICC1* variants harboring an additional *PKD2* or *PKD1* variant *in trans*, respectively. None of these *BICC1* variants were detected in the control cohort or in non-VEO-ADPKD patients (**Supplementary Material**). Moreover, besides the variants reported below, the patients had no other variants in any of other PKD genes or genes which phenocopy PKD including PKD1, PKD2, PKHD1, HNF1ß, GANAB, IFT140, DZIP1L, CYS1, DNAJB11, ALG5, ALG8, ALG9, LRP5, NEK8, OFD1, or PMM2. The first patient was severely and prenatally affected demonstrating a Potter sequence with huge echogenic kidneys and oligo-/anhydramnios. Autopsy confirmed VEO-ADPKD with absence of ductal plate malformation invariably seen in ARPKD. The fetus carried the *BICC1* variant (c.2462G>A, p.Gly821Glu) inherited from his father, who presented with two small renal cysts in one of his kidneys, and a *PKD2* variant (c.1894T>C, p.Cys632Arg) that arose *de novo* (**Fig. 5a**). Individual *in silico* predictions (SIFT, Polyphen2, CADD, Eigen-PC, FATHMM, GERP++ RS and EVE), meta scores (REVEL, MetaSVM, and MetaLR) and other protein function predictions (PrimateAI, Alphamissense, ESM1b and ProtVar) indicate that this PKD2 missense variant is likely pathogenic (**Supplementary Table S1**). Moreover, structural analysis suggests that the hydrophilic substitution may interfere with the Helix S5 pore domain of PKD2 and change its ion channel function (**Fig. 5b,c**). Finally, PKD2 p.Cys632Arg has been previously

reported as part of a PKD2 pedigree and implicated as a critical determinant for Polycystin-2 function.[42,43] On the other hand, the BICC1 p.Gly821Glu variant is located in an intrinsically disordered domain of BICC1 between the KH and the SAM domains (**Fig. 6f**). To address whether the variant is hypomorphic, we used CRISPR-Cas9-mediated gene editing to generate HEK293T cells lacking BICC1 or harboring the G821E mutation. These cells were analyzed for their impact on the translation of *PKD2*, a well-established target of Bicc1.[22] As shown in **Fig. 5d,e** PC2 protein levels were strongly reduced in two independent HEK293T BICC1 (G821E) cells when compared to unedited HEK293T cells. Most notably, the PC2 levels were comparable to the levels found in HEK293T carrying a BICC1 null allele (HEK293T BICC1 KO). Based on these data we hypothesize that the major disease effect results from the pathogenic *PKD2* variant but is aggravated by the BICC*1* variant.

The second patient presented perinatally with massively enlarged hyperechogenic kidneys, while the parents, both in their thirties, and the remaining family members were reported to be healthy (**Fig. 5f-h**). He carried a paternal canonic *BICC1* pathogenic splicing variant *(*c.1179+1G>T), which is likely pathogenic as the protein is truncated after exon 10, and a novel heterozygous *PKD1* variant (c.11942C>T, p.Ala3981Val) which has not been previously reported (**Fig. 5f**). While the Polycystin-1 variant appears minor in its amino acid change (i.e. Ala to Val), *in silico* analyses using individual predictions (SIFT, Polyphen2, CADD and EVE), Meta scores (REVEL) and other protein function predictions (PrimateAI, Alphamissense and ESM1b) indicate that missense variant is likely pathogenic (**Supplementary Table S1**). Structural analyses suggest that the Ala3981Val variant may not destabilize the Helix structure but may contact the TOP domain and interfere with domain flexibility and PC1 complex assembly.

**A Sibling Pair of PKD Patients with a Homozygous *BICC1* Mutation**

The most insightful finding for a critical role for BICC1 in human PKD was the discovery of a homozygous *BICC1* variant in a consanguinous Arab multiplex pedigree, two siblings, a boy and a girl, diagnosed with VEO-ADPKD (**Fig. 6a-e**). The affected female presented at a few months of age with kidney failure and enlarged polycystic kidneys that lacked corticomedullary differentiation. Histology after bilateral nephrectomy

showed polycystic kidneys more suggestive of ADPKD than ARPKD without any dysplastic element (**Fig. 6c**). Her younger brother exhibited enlarged hyperechogenic polycystic kidneys antenatally by ultrasound (**Fig. 6b**). In addition, during early infancy, arterial hypertension and a Dandy-Walker malformation with a low-pressure communicating hydrocephalus were noted (**Fig. 6d,e**). By customized MPS, we identified the homozygous evolutionarily well-conserved missense variant (c.718T>C, p.Ser240Pro) in *BICC1* (**Fig. 6a**). This variant was absent from gnomAD and perfectly segregated with the cystic phenotype present in this family. It results in a non-conservative change from the aliphatic, polar-hydrophilic serine to the cyclic, apolar-hydrophobic proline located in the second beta sheet of the first KHL1 domain and very likely disrupts the beta sheet and thus the RNA-binding activity of Bicc1 (**Fig. 6f,g** and **Supplementary Table S2**). In the more severely affected younger brother, we also detected the heterozygous *PKD2* change (c.1445T>G, p.Phe482Cys), which results in a non-conservative change from phenylalanine to cysteine (**Supplementary Table S1)**. It was previously reported that this Phe482Cys variant exhibited altered kinetic PC2 channel properties, increased expression in IMCD cells and a different subcellular distribution when compared to wild-type PC2,[44] These features suggested altered properties of this PC2 variant, yet its contribution to the case reported here remain untested.

Unfortunately, both siblings passed away and besides DNA and the phenotypic analysis described above neither human tissue nor primary patient-derived cells could be collected. Thus, to validate the pathogenicity of this point mutation, we turned to the amphibian model of PKD.[21,22] In *Xenopus*, knockdown of Bicc1 using antisense morpholino oligomers (*Bicc1-MO1+2*) causes a PKD phenotype, which can be rescued by co-injection of synthetic mRNA encoding *Bicc1*.[21] To test whether *BICC1* p.(Ser240Pro) has lost its biological activity, we introduced the same mutation into the *Xenopus* gene (*BicC1* S236P*). *Xenopus* embryos were injected with *Bicc1-MO1+2* at the 2-4 cell stage followed by a single injection of 2 ng wild type or *Bicc1* S236P* mRNAs at the 8-cell stage. At stage 39 (when kidney development has been completed) embryos were analyzed by whole mount *in situ* hybridization for the expression of *Nbc1* in the late distal tubule of the pronephric kidney, one of the most reliable readouts for the amphibian PKD

phenotype.[21] As shown in **Fig. 6h**, wild type *Bicc1* mRNA restored expression of *Nbc1* on the injected side in 63% of the embryos. However, *Bicc1* S236P* did not have any effect and the embryos were indistinguishable from those injected with the *Bicc1-MO1+2* alone. This suggested that *Bicc1* S236P* was functionally impaired. To address this hypothesis, we first assessed the subcellular localization of Bicc1 to foci that are thought to be involved in mRNA processing.[19,22,45] Transfection of Flag-tagged Bicc1 into HEK293T cells reproduced this pattern (**Fig. 6i**). Surprisingly, Bicc1 S236P-Flag was no longer detected in these cytoplasmic foci but rather homogenously dispersed throughout the cytoplasm (**Fig. 6j**). Western blot analysis demonstrated that this was accompanied by a reduction in protein levels (**Fig. 6k**). *In vitro* transcription/translation detected no differences between the proteins suggesting that the wildtype and Bicc1 S236P-Flag are translated equivalently (data not shown). Yet, in an *in vivo* pulse-chase experiments the S240P variant was less stable than its wildtype counterpart (**Fig. 6k**). However, whether the reduced protein level was due to an inherent instability of the mutant protein or a consequence of its mislocalization remains to be resolved. Finally, as in the case of *BICC1* G821E we engineered HEK293T cells to harbor the BICC1 S240P mutation. Western blot analysis demonstrated a strong reduction of PC2 levels in the BICC1 S240P cells when compared to unedited cells and that the PC2 levels were comparable to the BICC1 KO cells (**Figs. 5d,e** and **6l**).

Finally, to determine to what extent the *BICC1* S240P variant differs from a BICC1 loss of function, we performed mRNA sequencing (mRNA-seq) of the genetically engineered HEK293T cells. Differential gene expression analysis identified several genes that were differentially up- or down-regulated in the BICC1 S240P and the BICC1 KO cells compared to their unedited counterpart (**Supplementary Fig. 4a,e**). Approximately 24% and 18% of the differentially expressed genes were shared between BICC1 S240P or the KO cells, respectively (**Supplementary Fig. S4b,f**). Yet, a substantial number of genes were specific to either cell line. The BICC1 S240P-enriched/depleted transcripts were generally also enriched/depleted in the BICC1 KO cells, but did not reach statistical significance (**Supplementary Fig. 4c,g**). Conversely, many of the BICC1 KO enriched transcripts were specifically enriched/depleted in the

BICC1 KO cells and not in the BICC1 S240P cells (**Fig. 6m** and **Supplementary Fig. 4d**). This suggested that there are qualitative differences between a null phenotype and the BICC1 S240P variant, supporting our hypothesis that BICC1 S240P acts as a hypomorph. Indeed, Gene Set Enrichment Analysis (GSEA) using the hallmark gene sets and comparing BICC1 KO and S240P cells revealed a statistically significant enrichment for the Hallmark_Epithelial_Mesenchymal_Transition set (**Fig. 6n** and **Supplementary Table S3**), a pathway previously implicated in ADPKD.[46,47]

## DISCUSSION

In this study, we implicate BICC1 in the pathogenesis of human PKD by identifying the homozygous *BICC1 S240P* variant, which was sufficient to cause a cystic phenotype in a sibling pair of human PKD patients. While such a situation is extremely rare and does not significantly contribute to the mutational load in ADPKD or ARPKD, it demonstrated that loss of BICC1 is sufficient to cause PKD in humans. It is noteworthy that another study identified heterozygous *BICC1* mutations in two patients with mildly cystic dysplastic kidneys.[48] Yet, the variants were both also present in one of the parents, who were healthy questioning whether these findings could account for the cystic phenotype.

The second important aspect of this study is the co-segregation of variants in *BICC1* and *PKD1 and PKD2* in PKD patients from an International Clinical Diagnostic Cohort. We show that the *BICC1* G821E variant exhibits reduced PC2 expression when present in a homozygous state. While we have not yet shown the pathogenesis of the variants when introduced as a compound situation, we postulate that PKD alleles *in trans* and/or *de novo* exert an aggravating effect and contribute to polycystic kidney disease. A reduced dosage of PKD proteins would severely disturb the homeostasis and network integrity, and by this correlates with disease severity in PKD. ADPKD is quite heterogeneous and - even within the same family - shows quite some phenotypic variation.[49,50] It is thought that stochastic inputs, environmental factors and genetics influence PKD.[50] The demonstrated interaction of BICC1, PC1 and PC2 now provides a molecular mechanism that can explain some of the phenotypic variability in these families. Moreover, our animal studies suggest that this interaction promotes cyst formation and

augments the progression towards end-stage renal disease. Of note, while our mouse studies support the cooperation between Bicc1, Pkd1 and Pkd2, the genetic proof for Bicc1 acting as a disease modifier, i.e. reduction of Bicc1 activity in a Pkd1 or Pkd2 mutant background is still outstanding.BICC1 is ideally suited to modulate the PKD severity. Functional studies reported here and previously[22,30,31] demonstrate that BICC1 regulates the expression of PKD1, PKD2 and PKHD1. Integrating this with the fact that BICC1 and PC1/PC2 physically interact, we postulate that BICC1 acts as a feed-forward regulator to maintain PKD protein expression (see model in **Fig. 4k,l**). BICC1 functions as a posttranscriptional regulator modifying gene expression modulating the effects of microRNAs (miRNAs), regulating mRNA polyadenylation and translational repression and activation (with PKD2 being so far the sole activated target) [22,23,27,51-54]. In particular, the connection of BICC1 with miRNAs may have widespread consequences as a connection between miRNA activity and PKD is well-established [55-60] and is even considered as a PKD therapeutic.[61]

## DISCLOSURE STATEMENT

All the authors declared no competing interests.

## DATA SHARING STATEMENT

The datasets are presented in the figures and the supplementary information. The mRNA-seq data are deposited into the Gene Expression Omnibus (GEO) database (GSE262417) and are available online. Additional information is available from the corresponding author on reasonable request.

## ACKNOWLEDGMENTS

The authors would like to thank the patients and their families for their cooperation and interest in the study. This work was supported by grants from NIH/NIDDK (R01DK080745) and a philanthropic gift for PKD research at CCF to OW, Kidney Research UK and the PKD Charity UK (PKD_RP_005_20211124), the Sheffield Hospitals Charity and the Sheffield Kidney Research Foundation to AJS and ACMO, the Medical Research Council and the National Institute for Health and Care Research (NIHR) to ACMO

through the UK Renal Ciliopathies National Network (CILIAREN, grant agreement MR/Y007808/1), the Deutsche Forschungsgemeinschaft (DFG, BE 3910/8-2, BE 3910/9-1, Project-ID 431984000 - Collaborative Research Center SFB 1453), the Federal Ministry of Education and Research (BMBF, 01GM1903I and 01GM1903G) and the European Union's Horizon Europe research and innovation programme (grant agreement 101080717, TheRaCil) to CB. DS was supported by a Faculty PhD Scholarship from the University of Sheffield. We thank Drs. S. Somlo, P. Igarashi, and K. Dell for mouse strains, S. Feng, and L. Chang for technical and R. Allen Schweickart for bioinformatical support.

## SUPPLEMENTARY MATERIAL

### Supplementary Figure Legends

**Supplementary Figure S1. Validation of BICC1 Knockout and *Xenopus* Knockdowns.** (**a**) qRT-PCR for BICC1 comparing wildtype cells to the two genetically engineered BICC1 knockout clones. (**b**) qRT-PCR detecting the region targeted by the *Pkhd1-sMO* using a PrimeTime® qPCR assay (IDT). *Xenopus* embryos were injected with the indicated amount of *Pkhd1-sMO* and harvested at stage 39 for mRNA extraction. Individual dots indicate pools of 5 embryos each utilizing three independent fertilizations. Data were analyzed by Mann Whitney test with one asterisk indicating $P \leq 0.05$ and two asterisks indicating $P \leq 0.01$. (**c**). To examine cooperativity between Bicc1 and the PKD genes, each MO was titrated for efficacy alone or tested in combination. Embryos were analyzed for edema formation at stage 43. Data are accumulation of multiple independent fertilizations with N > 30 for each condition. Part of the data are shown in **Fig. 3j**.

**Supplementary Figure S2. *In vitro* Binding Assays Showing Direct Binding between Bicc1, PC1-PLAT and PC1-CT1, but not PC2-CT2.** *In vitro* translated myc-Bicc1 was incubated with recombinant MBP, MBP-PLAT and MBP-CT1 or GST, GST-CT2 and subjected to IP with anti-c-myc antibody. Arrows indicate pull down of MBP-PLAT and MBP-CT1 respectively; asterisk indicates non-specific band (**a**) or via GST pulldown (**b**). Quality of the different recombinant proteins used was confirmed by Coomassie

staining (**c**). Western blot analysis following Co-IP experiments, using GST tagged constructs as bait, identified protein interactions between GST-PC1 CT domain and *Bicc1*. GST was included as a negative control (**d**).

**Supplementary Figure S3. Kidney Parameters of *Bicc1:Pkd2* and *Bicc1:Pkd1* Compound Mutants.** (**a,b**) Comparison of Blood Urea Nitrogen (BUN) levels of kidneys of the *Bicc1:Pkd2* crosses at postnatal day P14 and P21. (**c,d**) Comparison of kidney weight/body weight ratios (KW/BW) levels of kidneys of *Bicc1:Pkd1* crosses and their respective BUN levels at postnatal day P14. (**e**) Immunoprecipitation of PC2 from kidneys of $Bicc1^{+/+}$ and $Bicc1^{Bpk/Bpk}$ mice at postnatal day P4. 200 μg total protein from each sample was used to immunoprecipitate PC2 with 5 μg Ycc2 antibody and agarose-bound protein A/G. PC2 was detected using another antibody against Pkd2 (Sc-28331).

**Supplementary Figure S4. Transcriptomic Analysis of BICC1 Wildtype, Knockout and S240P HEK293T cells.** (**a-g**) mRNA-seq data were analyzed using DESeq2 differential expression analysis using two samples per genotype. Venn Diagrams were used to visualize the distribution of the up- or downregulated transcripts (**a, e**); for each intersection the eight most significantly altered transcripts (based on their $P_{adj}$ levels) are visualized in a bar diagram showing the normalized expression levels for each sample (**b-d,f,g**).

**Supplementary Table S1: *In Silico* Analysis of the *PKD1* and *PKD2* Variants Identified in VEO-ADPKD Patients.**

**Supplementary Table S2. *In Silico* Analysis of the *S240P BICC1* Variant.**

**Supplementary Table S3: Gene Sets Enriched in BICC1 KO *vs.* BICC1 S240P HEK293T Cells.**

**Supplementary Methods**

**Supplementary References**

**Supplementary information is available on Kidney International's website.**

## REFERENCES


1. Harris PC, Torres VE. Polycystic kidney disease. Review. *Annu Rev Med*. 2009;60:321-337. doi:10.1146/annurev.med.60.101707.125712
2. Ong AC, Devuyst O, Knebelmann B, Walz G, Diseases E-EWGfIK. Autosomal dominant polycystic kidney disease: the changing face of clinical management. *Lancet*. May 16 2015;385(9981):1993-2002. doi:10.1016/S0140-6736(15)60907-2
3. Torres VE, Harris PC, Pirson Y. Autosomal dominant polycystic kidney disease. *Lancet*. 2007/04/14/ 2007;369(9569):1287-1301. doi:10.1016/S0140-6736(07)60601-1
4. Bergmann C, Guay-Woodford LM, Harris PC, Horie S, Peters DJM, Torres VE. Polycystic kidney disease. *Nat Rev Dis Primers*. Dec 6 2018;4(1):50. doi:10.1038/s41572-018-0047-y
5. Bergmann C, Zerres K. Early manifestations of polycystic kidney disease. *Lancet*. 2007/06/30/ 2007;369(9580)doi:10.1016/S0140-6736(07)61005-8
6. Ogborn MR. Polycystic kidney disease--a truly pediatric problem. *Pediatr Nephrol*. Dec 1994;8(6):762-767. doi:10.1007/BF00869116
7. Rossetti S, Kubly VJ, Consugar MB, et al. Incompletely penetrant PKD1 alleles suggest a role for gene dosage in cyst initiation in polycystic kidney disease. *Kidney Int*. Apr 2009;75(8):848-855. doi:10.1038/ki.2008.686
8. Vujic M, Heyer CM, Ars E, et al. Incompletely penetrant PKD1 alleles mimic the renal manifestations of ARPKD. *J Am Soc Nephrol*. Jul 2010;21(7):1097-1102. doi:10.1681/ASN.2009101070
9. **Bergmann C**. ARPKD and early manifestations of ADPKD: the original polycystic kidney disease and phenocopies. *Pediatric nephrology*. Mar 1 2014;doi:10.1007/s00467-013-2706-2
10. Durkie M, Chong J, Valluru MK, Harris PC, Ong ACM. Biallelic inheritance of hypomorphic PKD1 variants is highly prevalent in very early onset polycystic kidney disease. *Genet Med*. Apr 2021;23(4):689-697. doi:10.1038/s41436-020-01026-4
11. Ong AC, Harris PC. A polycystin-centric view of cyst formation and disease: the polycystins revisited. *Kidney Int*. Oct 2015;88(4):699-710. doi:10.1038/ki.2015.207
12. Senum SR, Li YSM, Benson KA, et al. Monoallelic IFT140 pathogenic variants are an important cause of the autosomal dominant polycystic kidney-spectrum phenotype. *Am J Hum Genet*. Jan 6 2022;109(1):136-156. doi:10.1016/j.ajhg.2021.11.016
13. Besse W, Chang AR, Luo JZ, et al. ALG9 Mutation Carriers Develop Kidney and Liver Cysts. *J Am Soc Nephrol*. Nov 2019;30(11):2091-2102. doi:10.1681/ASN.2019030298
14. Cornec-Le Gall E, Olson RJ, Besse W, et al. Monoallelic Mutations to DNAJB11 Cause Atypical Autosomal-Dominant Polycystic Kidney Disease. *Am J Hum Genet*. May 3 2018;102(5):832-844. doi:10.1016/j.ajhg.2018.03.013
15. Porath B, Gainullin VG, Cornec-Le Gall E, et al. Mutations in GANAB, Encoding the Glucosidase IIalpha Subunit, Cause Autosomal-Dominant Polycystic Kidney and Liver Disease. *Am J Hum Genet*. Jun 2 2016;98(6):1193-1207. doi:10.1016/j.ajhg.2016.05.004
16. Nauta J, Ozawa Y, Sweeney WE, Jr., Rutledge JC, Avner ED. Renal and biliary abnormalities in a new murine model of autosomal recessive polycystic kidney disease. *Pediatric nephrology*. Apr 1993;7(2):163-172.
17. Flaherty L, Bryda EC, Collins D, Rudofsky U, Montogomery JC. New mouse model for polycystic kidney disease with both recessive and dominant gene effects. *Kidney Int*. Feb 1995;47(2):552-558.
18. Cogswell C, Price SJ, Hou X, Guay-Woodford LM, Flaherty L, Bryda EC. Positional cloning of jcpk/bpk locus of the mouse. *Mamm Genome*. Apr 2003;14(4):242-249.
19. Maisonneuve C, Guilleret I, Vick P, et al. Bicaudal C, a novel regulator of Dvl signaling abutting RNA-processing bodies, controls cilia orientation and leftward flow. *Development*. Sep 2009;136(17):3019-3030. doi:136/17/3019 [pii]

10.1242/dev.038174

20. Bouvrette DJ, Sittaramane V, Heidel JR, Chandrasekhar A, Bryda EC. Knockdown of bicaudal C in zebrafish (Danio rerio) causes cystic kidneys: a nonmammalian model of polycystic kidney disease. Research Support, N.I.H., Extramural
Research Support, Non-U.S. Gov't. *Comparative medicine*. Apr 2010;60(2):96-106.
21. Tran U, Pickney LM, Ozpolat BD, Wessely O. Xenopus Bicaudal-C is required for the differentiation of the amphibian pronephros. *Dev Biol*. Jul 1 2007;307(1):152-164. doi:10.1016/j.ydbio.2007.04.030
22. Tran U, Zakin L, Schweickert A, et al. The RNA-binding protein bicaudal C regulates polycystin 2 in the kidney by antagonizing miR-17 activity. *Development*. Apr 2010;137(7):1107-1116. doi:10.1242/dev.046045
23. Dowdle ME, Kanzler CR, Harder CRK, Moffet S, Walker MN, Sheets MD. Bicaudal-C Post-transcriptional regulator of cell fates and functions. *Front Cell Dev Biol*. 2022;10:981696. doi:10.3389/fcell.2022.981696
24. Wessely O, Tran U, Zakin L, De Robertis EM. Identification and expression of the mammalian homologue of Bicaudal-C. *Mech Dev*. Mar 2001;101(1-2):267-270.
25. Wessely O, De Robertis EM. The Xenopus homologue of Bicaudal-C is a localized maternal mRNA that can induce endoderm formation. *Development*. May 2000;127(10):2053-2062.
26. Mahone M, Saffman EE, Lasko PF. Localized *Bicaudal-C* RNA encodes a protein containing a KH domain, the RNA binding motif of FMR1. *EMBO J*. 1995 May 1 1995;14(9):2043-2055.
27. Piazzon N, Maisonneuve C, Guilleret I, Rotman S, Constam DB. Bicc1 links the regulation of cAMP signaling in polycystic kidneys to microRNA-induced gene silencing. *Journal of molecular cell biology*. Jul 3 2012;doi:10.1093/jmcb/mjs027
28. Kilkenny C, Browne WJ, Cuthill IC, Emerson M, Altman DG. Improving bioscience research reporting: the ARRIVE guidelines for reporting animal research. *PLoS Biol*. Jun 29 2010;8(6):e1000412. doi:10.1371/journal.pbio.1000412
29. Lian P, Li A, Li Y, et al. Loss of polycystin-1 inhibits Bicc1 expression during mouse development. *PLoS One*. 2014;9(3):e88816. doi:10.1371/journal.pone.0088816
30. Lemaire LA, Goulley J, Kim YH, et al. Bicaudal C1 promotes pancreatic NEUROG3+ endocrine progenitor differentiation and ductal morphogenesis. *Development*. Mar 1 2015;142(5):858-870. doi:10.1242/dev.114611
31. Mesner LD, Ray B, Hsu YH, et al. Bicc1 is a genetic determinant of osteoblastogenesis and bone mineral density. *J Clin Invest*. Jun 2 2014;124(6):2736-2749. doi:10.1172/JCI73072
32. Xu Y, Streets AJ, Hounslow AM, et al. The Polycystin-1, Lipoxygenase, and alpha-Toxin Domain Regulates Polycystin-1 Trafficking. *J Am Soc Nephrol*. Apr 2016;27(4):1159-1173. doi:10.1681/ASN.2014111074
33. Onuchic LF, Furu L, Nagasawa Y, et al. PKHD1, the polycystic kidney and hepatic disease 1 gene, encodes a novel large protein containing multiple immunoglobulin-like plexin-transcription-factor domains and parallel beta-helix 1 repeats. *Am J Hum Genet*. May 2002;70(5):1305-1317.
34. Vick P, Kreis J, Schneider I, et al. An Early Function of Polycystin-2 for Left-Right Organizer Induction in Xenopus. *iScience*. Apr 27 2018;2:76-85. doi:10.1016/j.isci.2018.03.011
35. Xu Y, Streets AJ, Hounslow AM, et al. The Polycystin-1, Lipoxygenase, and alpha-Toxin Domain Regulates Polycystin-1 Trafficking. *J Am Soc Nephrol*. Aug 26 2015;doi:10.1681/ASN.2014111074
36. Wu G, Markowitz GS, Li L, et al. Cardiac defects and renal failure in mice with targeted mutations in Pkd2. *Nat Genet*. Jan 2000;24(1):75-78.
37. Wu G, Tian X, Nishimura S, et al. Trans-heterozygous Pkd1 and Pkd2 mutations modify expression of polycystic kidney disease. *Hum Mol Genet*. Aug 1 2002;11(16):1845-1854.
38. Nauta J, Ozawa Y, Sweeney WE, Jr., Rutledge JC, Avner ED. Renal and biliary abnormalities in a new murine model of autosomal recessive polycystic kidney disease. Research Support, Non-U.S. Gov't
Research Support, U.S. Gov't, P.H.S. *Pediatr Nephrol*. Apr 1993;7(2):163-172.

39. Williams SS, Cobo-Stark P, Hajarnis S, et al. Tissue-specific regulation of the mouse Pkhd1 (ARPKD) gene promoter. *Am J Physiol Renal Physiol*. Aug 1 2014;307(3):F356-368. doi:10.1152/ajprenal.00422.2013
40. Devane J, Ott E, Olinger EG, et al. Progressive liver, kidney, and heart degeneration in children and adults affected by TULP3 mutations. *Am J Hum Genet*. May 5 2022;109(5):928-943. doi:10.1016/j.ajhg.2022.03.015
41. Lu H, Galeano MCR, Ott E, et al. Mutations in DZIP1L, which encodes a ciliary-transition-zone protein, cause autosomal recessive polycystic kidney disease. *Nat Genet*. Jul 2017;49(7):1025-1034. doi:10.1038/ng.3871
42. Magistroni R, He N, Wang K, et al. Genotype-renal function correlation in type 2 autosomal dominant polycystic kidney disease. *JASN*. 2003;14(5):1164-1174.
43. Feng S, Rodat-Despoix L, Delmas P, Ong AC. A single amino acid residue constitutes the third dimerization domain essential for the assembly and function of the tetrameric polycystin-2 (TRPP2) channel. *J Biol Chem*. May 27 2011;286(21):18994-19000. doi:10.1074/jbc.M110.192286
44. Dedoussis GV, Luo Y, Starremans P, et al. Co-inheritance of a PKD1 mutation and homozygous PKD2 variant: a potential modifier in autosomal dominant polycystic kidney disease. *Eur J Clin Invest*. Mar 2008;38(3):180-190. doi:10.1111/j.1365-2362.2007.01913.x
45. Stagner EE, Bouvrette DJ, Cheng J, Bryda EC. The polycystic kidney disease-related proteins Bicc1 and SamCystin interact. *Biochem Biophys Res Commun*. May 22 2009;383(1):16-21. doi:S0006-291X(09)00599-3 [pii]
10.1016/j.bbrc.2009.03.113
46. Kim DY, Woo YM, Lee S, et al. Impact of miR-192 and miR-194 on cyst enlargement through EMT in autosomal dominant polycystic kidney disease. *FASEB J*. Feb 2019;33(2):2870-2884. doi:10.1096/fj.201800563RR
47. Formica C, Peters DJM. Molecular pathways involved in injury-repair and ADPKD progression. *Cell Signal*. Aug 2020;72:109648. doi:10.1016/j.cellsig.2020.109648
48. Kraus MR, Clauin S, Pfister Y, et al. Two mutations in human BICC1 resulting in Wnt pathway hyperactivity associated with cystic renal dysplasia. *Hum Mutat*. Jan 2012;33(1):86-90. doi:10.1002/humu.21610
49. Milutinovic J, Rust PF, Fialkow PJ, et al. Intrafamilial phenotypic expression of autosomal dominant polycystic kidney disease. Research Support, U.S. Gov't, P.H.S. *American journal of kidney diseases : the official journal of the National Kidney Foundation*. May 1992;19(5):465-472.
50. Harris PC, Rossetti S. Determinants of renal disease variability in ADPKD. Review. *Advances in chronic kidney disease*. Mar 2010;17(2):131-139. doi:10.1053/j.ackd.2009.12.004
51. Wang L, Eckmann CR, Kadyk LC, Wickens M, Kimble J. A regulatory cytoplasmic poly(A) polymerase in Caenorhabditis elegans. *Nature*. Sep 19 2002;419(6904):312-316.
52. Chicoine J, Benoit P, Gamberi C, Paliouras M, Simonelig M, Lasko P. Bicaudal-C recruits CCR4-NOT deadenylase to target mRNAs and regulates oogenesis, cytoskeletal organization, and its own expression. *Dev Cell*. Nov 2007;13(5):691-704. doi:S1534-5807(07)00380-2 [pii]
10.1016/j.devcel.2007.10.002
53. Zhang Y, Park S, Blaser S, Sheets MD. Determinants of RNA binding and translational repression by the Bicaudal-C regulatory protein. *J Biol Chem*. Mar 14 2014;289(11):7497-7504. doi:10.1074/jbc.M113.526426
54. Zhang Y, Cooke A, Park S, Dewey CN, Wickens M, Sheets MD. Bicaudal-C spatially controls translation of vertebrate maternal mRNAs. *RNA*. Nov 2013;19(11):1575-1582. doi:10.1261/rna.041665.113
55. Chu AS, Friedman JR. A role for microRNA in cystic liver and kidney diseases. *J Clin Invest*. Nov 2008;118(11):3585-3587. doi:10.1172/JCI36870
56. Patel V, Williams D, Hajarnis S, et al. miR-17~92 miRNA cluster promotes kidney cyst growth in polycystic kidney disease. *Proc Natl Acad Sci USA*. Jun 25 2013;110(26):10765-10770. doi:10.1073/pnas.1301693110

57. Pandey P, Brors B, Srivastava PK, et al. Microarray-based approach identifies microRNAs and their target functional patterns in polycystic kidney disease. Research Support, Non-U.S. Gov't. *BMC Genomics*. 2008;9:624. doi:10.1186/1471-2164-9-624
58. Pandey P, Qin S, Ho J, Zhou J, Kreidberg JA. Systems biology approach to identify transcriptome reprogramming and candidate microRNA targets during the progression of polycystic kidney disease. Research Support, N.I.H., Extramural
Research Support, Non-U.S. Gov't. *BMC systems biology*. 2011;5:56. doi:10.1186/1752-0509-5-56
59. Patel V, Hajarnis S, Williams D, Hunter R, Huynh D, Igarashi P. MicroRNAs regulate renal tubule maturation through modulation of Pkd1. *J Am Soc Nephrol*. Dec 2012;23(12):1941-1948. doi:10.1681/ASN.2012030321
60. Nagalakshmi VK, Ren Q, Pugh MM, Valerius MT, McMahon AP, Yu J. Dicer regulates the development of nephrogenic and ureteric compartments in the mammalian kidney. *Kidney Int*. Feb 2011;79(3):317-330. doi:10.1038/ki.2010.385
61. Lee EC, Valencia T, Allerson C, et al. Discovery and preclinical evaluation of anti-miR-17 oligonucleotide RGLS4326 for the treatment of polycystic kidney disease. *Nat Commun*. Sep 12 2019;10(1):4148. doi:10.1038/s41467-019-11918-y

## FIGURE LEGENDS

**Figure 1. *Bicc1* Forms a Complex with Polycystin-1 and Polycystin-2.** Full-length and deletion myc-tagged constructs of Bicc1 were co-expressed with either full-length HA-tagged PC1 or PC2 in HEK-293 cells and tested for their ability to interact by co-IP. (**a**) Schematic diagram of the constructs used in this experiment. (**b**) Western blot analysis following co-IP experiments, using GST tagged constructs as bait, identified protein interactions between PC1 or PC2 domains and *Bicc1*. pcDNA3 was included as a negative control. CT = C-terminus, NT = N-terminus, GST = Glutathione S-Transferase. (**c**) Western blot showing expression of recombinant myc-tagged *Bicc1* generated by *in vitro* translation or myc-tagged *Bicc1* transfected in HEK-293 cells. (**d**) Western blot analysis following *in-vitro* pulldown experiments, using purified GST tagged constructs as bait, identified direct protein interactions between PC1 or PC2 domains and *in vitro* translated myc-Bicc1. (**e**) Western blot analysis following co-IP experiments, using a rabbit PC1 antibody (2b7) as bait, identified protein interactions between PC1 and Bicc1. A non-immune rabbit IgG antibody or no antibody was included as a negative control; * denotes the non-specific IgG band. (**f**) Western blot analysis following co-IP experiments, using an anti-mouse Bicc1 or anti-goat PC2 antibody as bait, identified protein interactions between PC2 and Bicc1. Non-immune goat and mouse IgG was included as a negative control.

**Figure 2. Interactions between *Bicc1* and Polycystin1/2 Require Different Binding Motifs.** Full-length and deletion myc-tagged constructs of Bicc1 were co-expressed with either full-length HA-tagged PC1 or PC2 in HEK-293 cells and tested for their ability to interact by co-IP. (**a**) Schematic diagram of the constructs used in this set of experiments. (**b,c**) Western blot analysis following co-IP experiments, using a PC1-HA-tagged construct as bait, identified protein interactions between PC1 and Bicc1 domains. pcDNA3 was included as a negative control (**b**). co-IP experiments (n=3) were quantified in (**c**). (**d,e**) Western blot analysis following co-IP experiments, using a PC2-HA tagged construct as bait, identified protein interactions between PC2 and Bicc1 domains (**d**). pcDNA3 was included as a negative control. Quantification of the co-IP experiments (n=3) is shown in (**e**). Two-sided paired t-tests were performed to

assess significance (*P* values * ≤ 0.05, ** = ≤ 0.01, *** = ≤ 0.001, **** = ≤ 0.0001 and ns = not significant). Error bars represent standard error of the mean.

**Figure 3**. **Cooperativity of Bicc1 and PKD Genes in *Xenopus*.** (**a-d**) mRNA expression of *Pkd1*, *Pkhd1, Pkd2* and *Bicc1* in the *Xenopus* pronephros at stage 39. (**e-i”**) Knockdown of Bicc1 (**f-f”**), Pkd1 (**g-g”**), Pkd2 (**h-h”**) and Pkhd1 (**i-i”**) by antisense morpholino oligomers (MOs) results in a PKD phenotype compared to uninjected control *Xenopus* embryos (**e-e”**). The phenotype is characterized by the formation of edema due to kidney dysfunction (**e,f,g,h,i**; stage 43), the development of dilated renal tubules (**e’,f’,g’,h’,i’**; stage 43) and the loss of *Nbc1* in the late distal tubule by whole mount *in situ* hybridizations (arrowheads in **e”,f”,g”,h”,i”**; stage 39). **(j,k)** To examine cooperativity, *Xenopus* embryos were injected with suboptimal amounts of the MOs, either alone or in combination, and analyzed for edema formation at stage 43 (**j**) and the expression of *Nbc1* at stage 39 (**k**). More than three independent experiments were analyzed. In (**k**), gray bars show reduced and black bars show absent expression of *Nbc1* in the late distal tubule. Data are the accumulation of multiple independent fertilizations with N>30 for each condition.

**Figure 4: Cooperativity of Bicc1 and Pkd1 and Pkd2 in Mouse.** (**a-d**) Bicc1 and Pkd2 interact genetically. Offspring from *Bicc1;Pkd2* compound mice at postnatal day P4 and P14 are compared by outside kidney morphology at postnatal day P14 (**a**), kidney weight at P14 (**b**) and kidney to body weight ratio (KW/BW) at P4 (**c**) and P14 (**d**). (**e-h**) Bicc1 and Pkd1 interact genetically. *Bicc1;Pkd1* compound mice are compared by outside kidney morphology at P14 (**e**), estimation plot of KW/BW ratio comparing littermates at P14 with a *P*-value = 0.092 (**f**), and cystic index of proximal tubules (PT) and collecting ducts (CD) at P7 (**g**) and P14 (**h**). Two-sided paired t-tests were performed to assess significance; one asterisk indicates a *P*-value of ≤ 0.05 and two asterisks a *P*-value of ≤ 0.01; error bars represent standard deviation. (**i,j**) qRT-PCR analysis for *Pkd1*, *Pkd2* and *Pkhd1* expression (**i**) and quantification of the PC2 expression levels determined by immunoprecipitation (**j**) in two wildtype and two Bicc1$^{Bpk/Bpk}$ littermates at P4 before the onset of a strong cystic kidney phenotype. PCR data were analyzed by 2-

way ANOVA with two asterisks indicating a *P*-value of ≤ 0.01 and three asterisks indicating a *P*-value ≤ 0.001. (**k,l**) Model for how the complex of BICC1, PC1 and PC2 self-regulates its expression in a feed-forward loop. See text for details. Generated with Biorender.com.

**Figure 5. Identification of Human *BICC1* Variants.** (**a-c**) BICC1 p.G821E/PKD2 p.C632R case with pedigree and the electropherograms (**a**), the structural analysis of the PKD2 showing the local structure around the cysteine at position 632 (indicated in red) and its putative impact in the variant including the REVEL score (**b**) as well as its location within the global PC2 structure highlighting the potential of the variant impacting the PC2 ion channel function (**c**). (**d,e**) Western blot analysis for PC2 comparing wildtype HEK293T, BICC1 G821E, BICC1 S240P and *BICC1* KO HEK293T and quantification thereof. γ-Tubulin was used as loading control. (**f-i**) BICC1 I1179+1G>T/PKD1 PKD1 p.Ala3981Val case with pedigree and the electropherograms (**f**), the ultrasound analysis of the left and right kidneys (**g,h**) and the structural analysis of the PC1 showing the local structure around the alanine at position 3981 (indicated in red) and its putative impact in the variant including the REVEL score (**i**).

**Figure 6: The Homozygous BICC1 S240P Mutation is a Hypomorphic Cystic Disease-Causing Variant.** (**a-e**) Consanguineous multiplex pedigree with two siblings affected by VEO-ADPKD identified the homozygous *BICC1* missense variant c.718T>C (p.S240P) absent from gnomAD and other internal and public databases. Electropherogram is shown in (**a**). The affected girl presented at a few months of age with renal failure and enlarged polycystic kidneys that lacked corticomedullary differentiation (**c**). Histology after bilateral nephrectomy showed polycystic kidneys more suggestive of ADPKD than ARPKD without any dysplastic element**.** Her younger brother exhibited enlarged hyperechogenic polycystic kidneys prenatally by ultrasound (**b**). In addition, in his early infancy arterial hypertension and a Dandy-Walker malformation with a low-pressure communicating hydrocephalus were noted (**d,e**). (**f**) Ribbon diagram and schematic diagram of BICC1 contains KH, KHL and SAM domains showing the variants discovered. (**g**) Solid boxes correspond to local impacts of p.S240P on BICC1 structure, interactions are labeled as dashed lines (pseudobonds). GXXG motifs colored in magenta, representative missense variant residues colored in

red and residues adjacent to selected variant (<5Å) colored in tan. (**h**) Rescue experiments of *Xenopus* embryos lacking BicC1 by co-injections with the wild type or mutant constructs. Embryos were scored for the re-expression of *Nbc1* in the late distal tubule by whole mount *in situ* hybridizations. Quantification of at least 3 independent experiments is shown. **(i,j**) HEK293T cells were transfected with Flag-tagged constructs of wild type or mutant Bicc1 and the subcellular localization of Bicc1 was visualized (red). Nuclei were counterstained with DAPI (blue). (**k**) Protein stability analysis using tetracycline-inducible HEK293T cells comparing the expression levels of Bicc1 and Bicc1(S240P) 24 hours after removal of tetracycline and addition of cycloheximide. γ-Tubulin was used as loading control. The percentage of protein destabilization because of protein synthesis inhibition by cycloheximide is indicated. (**l**) Western Blot analysis of wildtype HEK293T, cells lacking BICC1 ($BICC1^{-/-}$) and isogenic cells with the BICC1 S240P mutation for PC2 expression. GAPDH was used as loading control. (**m,n**) Bar graph of the mRNA-seq transcriptomic analysis comparing BICC1 wildtype, knockout and S240P isogenic HEK293T cells showing the eight most significantly upregulated transcripts (based on their $P_{adj}$ levels) in the BICC1 KO cells (**m**). For each gene, the normalized expression levels from each of the 6 samples (2 wildtype, KO and 240P each) is shown. (**n**) GSEA plot showing the enrichment of the Hallmark Epithelial_Mesenchymal_Transition data set in the BICC1 KO cells *vs.* the BICC1 S240P cells.

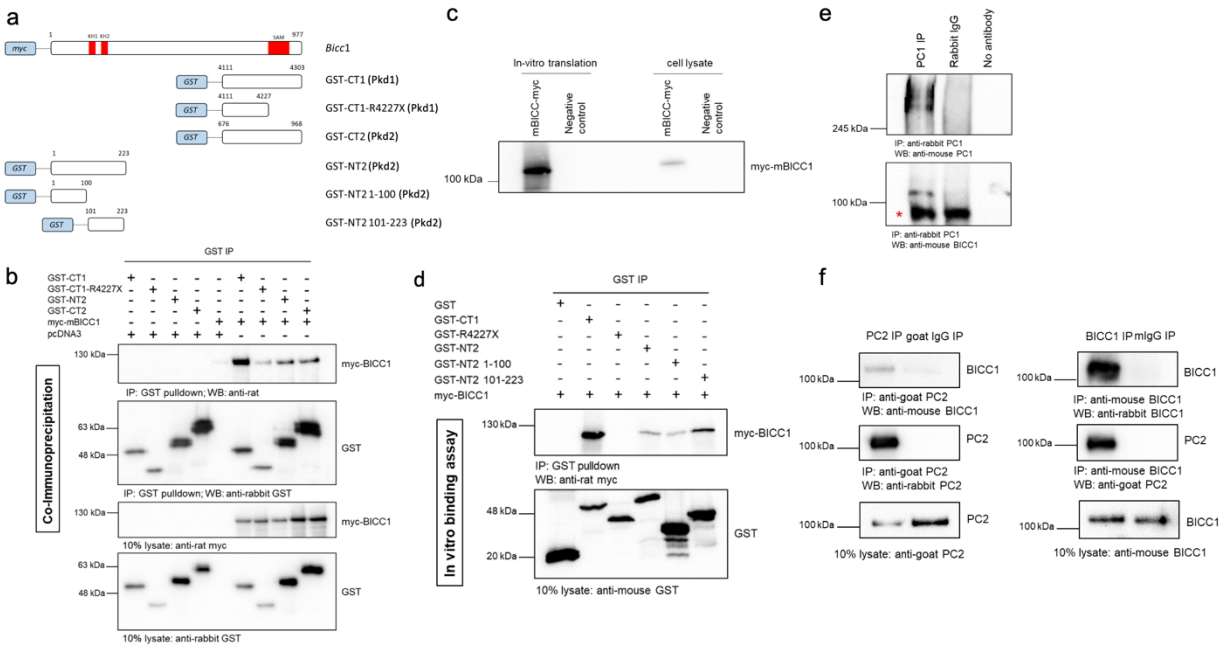


***Figure 1. Bicc1 Forms a Complex with Polycystin-1 and Polycystin-2.*** *Full-length and deletion myc-tagged constructs of Bicc1 were co-expressed with either full-length HA-tagged PC1 or PC2 in HEK-293 cells and tested for their ability to interact by co-IP. (**a**) Schematic diagram of the constructs used in this experiment. (**b**) Western blot analysis following co-IP experiments, using GST tagged constructs as bait, identified protein interactions between PC1 or PC2 domains and Bicc1. pcDNA3 was included as a negative control. CT = C-terminus, NT = N-terminus, GST = Glutathione S-Transferase. (**c**) Western blot showing expression of recombinant myc-tagged Bicc1 generated by in vitro translation or myc-tagged Bicc1 transfected in HEK-293 cells. (**d**) Western blot analysis following in-vitro pulldown experiments, using purified GST tagged constructs as bait, identified direct protein interactions between PC1 or PC2 domains and in vitro translated myc-Bicc1. (**e**) Western blot analysis following co-IP experiments, using a rabbit PC1 antibody (2b7) as bait, identified protein interactions between PC1 and Bicc1. A non-immune rabbit IgG antibody or no antibody was included as a negative control; * denotes the non-specific IgG band. (**f**) Western blot analysis following co-IP experiments, using an anti-mouse Bicc1 or anti-goat PC2 antibody as bait, identified protein interactions between PC2 and Bicc1. Non-immune goat and mouse IgG was included as a negative control.*

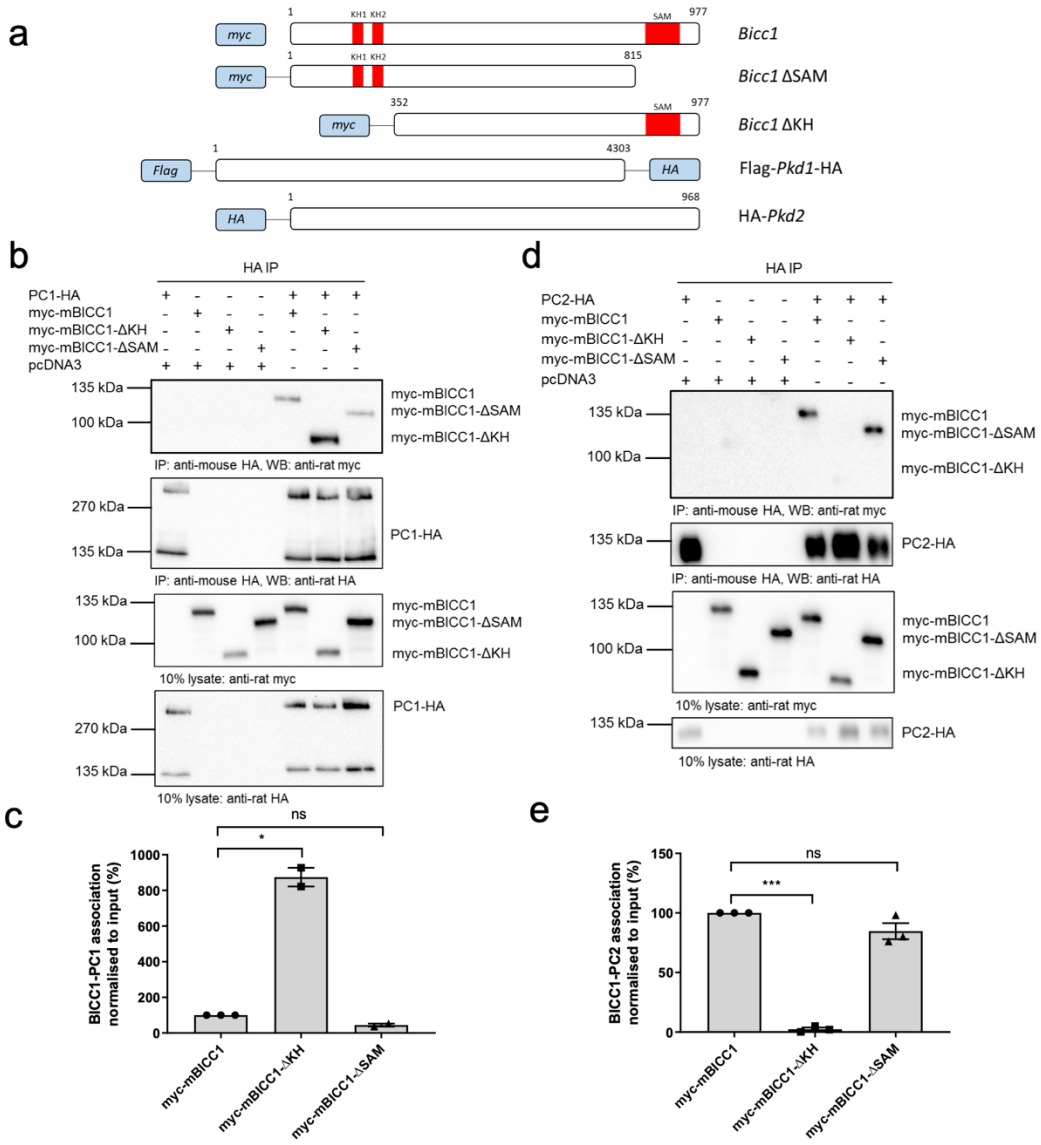


***Figure 2. Interactions between Bicc1 and Polycystin1/2 Require Different Binding Motifs.*** *Full-length and deletion myc-tagged constructs of Bicc1 were co-expressed with either full-length HA-tagged PC1 or PC2 in HEK-293 cells and tested for their ability to interact by co-IP. (**a**) Schematic diagram of the constructs used in this set of experiments. (**b,c**) Western blot analysis following co-IP experiments, using a PC1-HA-tagged construct as bait, identified protein interactions between PC1 and Bicc1 domains. pcDNA3 was included as a negative control (**b**). co-IP experiments (n=3) were quantified in (**c**). (**d,e**) Western blot analysis following co-IP experiments, using a PC2-HA tagged construct as bait, identified protein interactions between PC2 and Bicc1 domains (**d**). pcDNA3 was included as a negative control. Quantification of the co-IP experiments (n=3) are shown in (**e**). Two-sided paired t-tests were performed to assess significance (P values * ≤0.05, ** = ≤0.01, *** = ≤0.001, **** = ≤0.0001 and ns = not significant). Error bars represent standard error of the mean.*

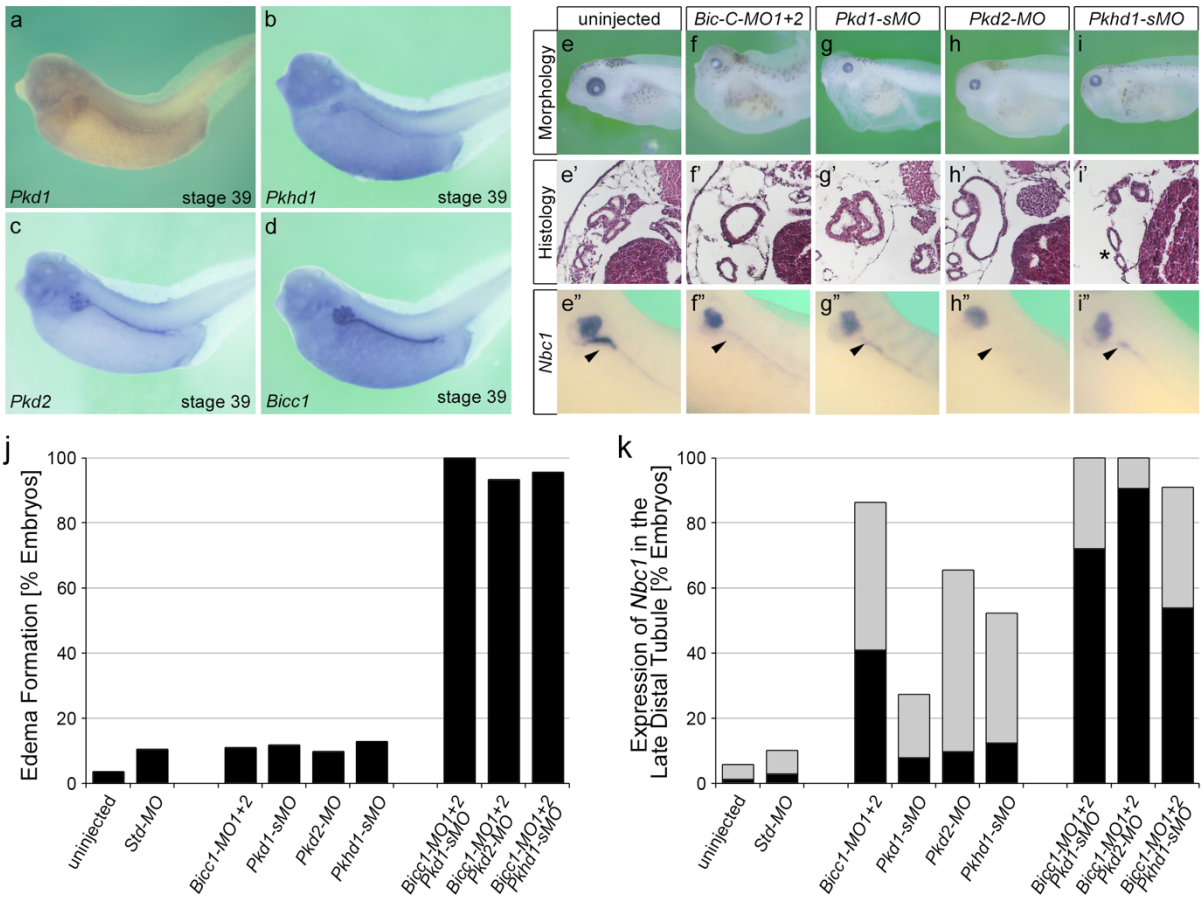


***Figure 3*. Cooperativity of Bicc1 and PKD Genes in Xenopus.** *(**a-d**) mRNA expression of Pkd1, Pkhd1, Pkd2 and Bicc1 in the Xenopus pronephros at stage 39. (**e-i"**) Knockdown of Bicc1 (**f-f"**), Pkd1 (**g-g"**), Pkd2 (**h-h"**) and Pkhd1 (**i-i"**) by antisense morpholino oligomers (MOs) results in a PKD phenotype compared to uninjected control Xenopus embryos (**e-e"**). The phenotype is characterized by the formation of edema due to kidney dysfunction (**e,f,g,h,i**; stage 43), the development of dilated renal tubules (**e',f',g',h',i'**; stage 43) and the loss of Nbc1 in the late distal tubule by whole mount in situ hybridizations (arrowheads in **e",f",g",h",i"**; stage 39). **(j,k)** To examine cooperativity, Xenopus embryos were injected with suboptimal amounts of the MOs, either alone or in combination, and analyzed for edema formation at stage 43 (**j**) and the expression of Nbc1 at stage 39 (**k**). More than three independent experiments were analyzed. In (**k**), gray bars show reduced and black bars show absent expression of Nbc1 in the late distal tubule. Data are the accumulation of multiple independent fertilizations with N>30 for each condition.*

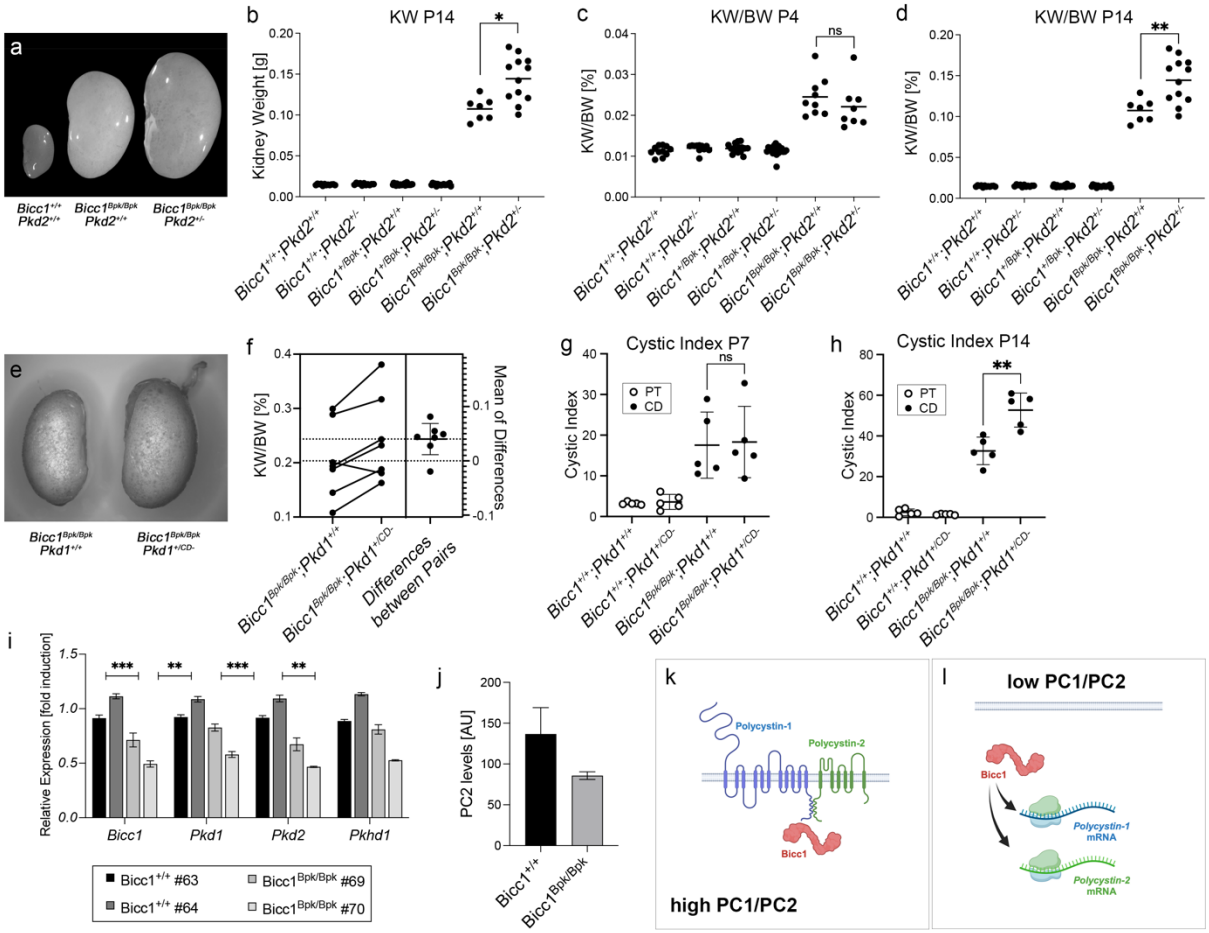


***Figure 4: Cooperativity of Bicc1 and Pkd1 and Pkd2 in Mouse.*** *(**a-d**) Bicc1 and Pkd2 interact genetically. Offspring from Bicc1;Pkd2 compound mice at postnatal day P4 and P14 are compared by outside kidney morphology at postnatal day P14 (**a**), kidney weight at P14 (**b**) and kidney to body weight ratio (KW/BW) at P4 (**c**) and P14 (**d**). (**e-h**) Bicc1 and Pkd1 interact genetically. Bicc1;Pkd1 compound mice are compared by outside kidney morphology at P14 (**e**), estimation plot of KW/BW ratio comparing littermates at P14 with a P-value = 0.092 (**f**), and cystic index of proximal tubules (PT) and collecting ducts (CD) at P7 (**g**) and P14 (**h**). Two-sided paired t-tests were performed to assess significance; one asterisk indicates a P-value of ≤ 0.05 and two asterisks a P-value of ≤ 0.01; error bars represent standard deviation. (**i,j**) qRT-PCR analysis for Pkd1, Pkd2 and Pkhd1 expression (**i**) and quantification of the PC2 expression levels determined by immunoprecipitation (**j**) in two wildtype and two Bicc1$^{Bpk/Bpk}$ littermates at P4 before the onset of a strong cystic kidney phenotype. PCR data were analyzed by 2-way ANOVA with two asterisks indicating a P-value of ≤ 0.01 and three asterisks indicating a P-value ≤ 0.001. (**k,l**) Model for how the complex of BICC1, PC1 and PC2 self-regulates its expression in a feed-forward loop. See text for details. Generated with Biorender.com.*

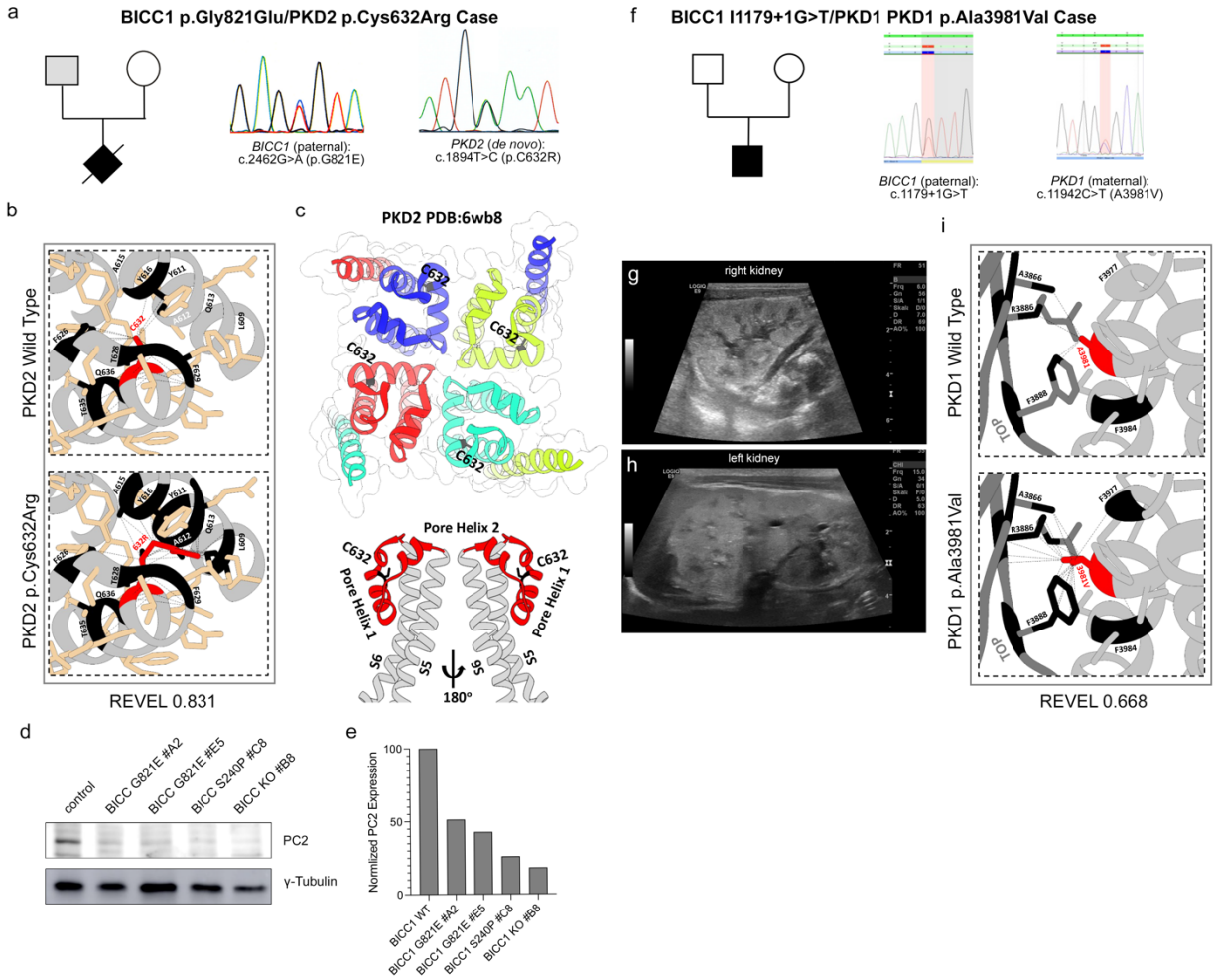


***Figure 5. Identification of Human BICC1 Variants.*** *(**a-c**) BICC1 p.G821E/PKD2 p.C632R case with pedigree and the electropherograms (**a**), the structural analysis of the PKD2 showing the local structure around the cysteine at position 632 (indicated in red) and its putative impact in the variant including the REVEL score (**b**) as well as its location within the global PC2 structure highlighting the potential of the variant impacting the PC2 ion channel function (**c**). (**d,e**) Western blot analysis for PC2 comparing wildtype HEK293T, BICC1 G821E, BICC1 S240P and BICC1 KO HEK293T and quantification thereof. g-Tubulin was used as loading control. (**f-i**) BICC1 I1179+1G>T/PKD1 PKD1 p.Ala3981Val case with pedigree and the electropherograms (**f**), the ultrasound analysis of the left and right kidneys (**g,h**) and the structural analysis of the PC1 showing the local structure around the alanine at position 3981 (indicated in red) and its putative impact in the variant including the REVEL score (**i**).*

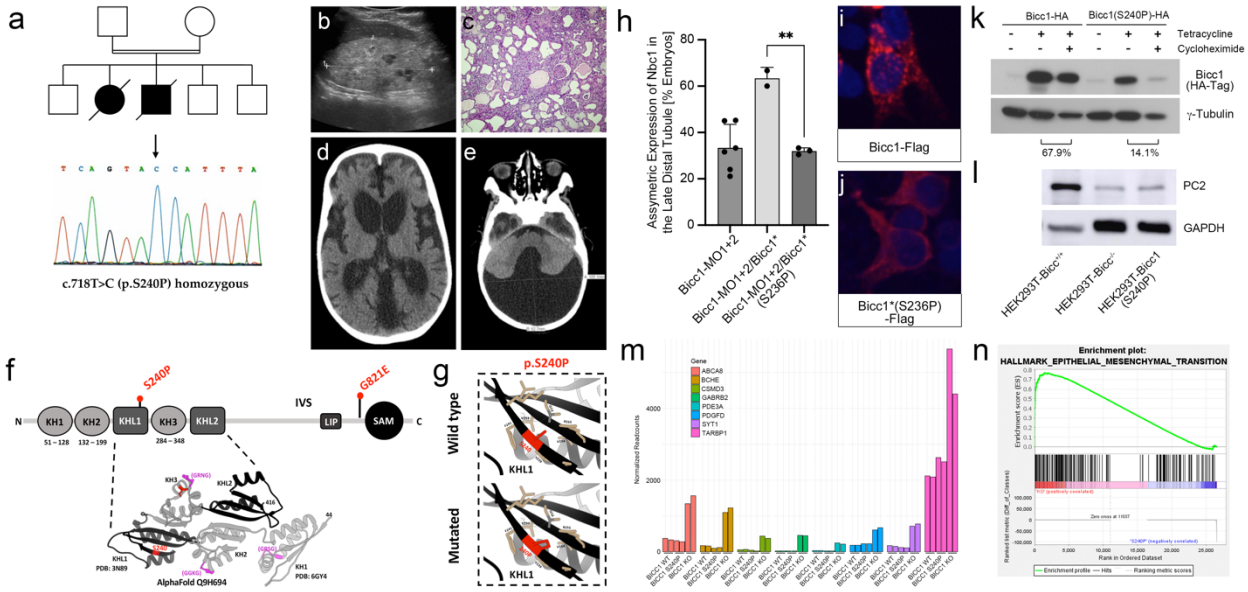


***Figure 6: The Homozygous BICC1 S240P Mutation is a Hypomorphic Cystic Disease-Causing Variant.*** *(**a-e**) Consanguineous multiplex pedigree with two siblings affected by VEO-ADPKD identified the homozygous BICC1 missense variant c.718T>C (p.S240P) absent from gnomAD and other internal and public databases. Electropherogram is shown in (**a**). The affected girl presented at a few months of age with renal failure and enlarged polycystic kidneys that lacked corticomedullary differentiation (**c**). Histology after bilateral nephrectomy showed polycystic kidneys more suggestive of ADPKD than ARPKD without any dysplastic element**.** Her younger brother exhibited enlarged hyperechogenic polycystic kidneys prenatally by ultrasound (**b**). In addition, in his early infancy arterial hypertension and a Dandy-Walker malformation with a low-pressure communicating hydrocephalus were noted (**d,e**). (**f**) Ribbon diagram and schematic diagram of BICC1 contains KH, KHL and SAM domains showing the variants discovered. (**g**) Solid boxes correspond to local impacts of p.S240P on BICC1 structure, interactions are labeled as dashed lines (pseudobonds). GXXG motifs colored in magenta, representative missense variant residues colored in red and residues adjacent to selected variant (<5Å) colored in tan. (**h**) Rescue experiments of Xenopus embryos lacking BicC1 by co-injections with the wild type or mutant constructs. Embryos were scored for the re-expression of Nbc1 in the late distal tubule by whole mount in situ hybridizations. Quantification of at least 3 independent experiments is shown. (**i,j**) HEK293T cells were transfected with Flag-tagged constructs of wild type or mutant Bicc1 and the subcellular localization of Bicc1 was visualized (red). Nuclei were counterstained with DAPI (blue). (**k**) Protein stability analysis using tetracycline-inducible HEK293T cells comparing the expression levels of Bicc1 and Bicc1(S240P) 24 hours after removal of tetracycline and addition of cycloheximide. ?-Tubulin was used as loading control. The percentage of protein destabilization because of protein synthesis inhibition by cycloheximide is indicated. (**l**) Western Blot analysis of wildtype HEK293T, cells lacking BICC1 (BICC1$^{-/-}$) and isogenic cells with the BICC1 S240P mutation for PC2 expression. GAPDH was used as loading control. (**m,n**) Bar graph of the mRNA-seq transcriptomic analysis comparing BICC1 wildtype, knockout and S240P isogenic HEK293T cells showing the eight most significantly upregulated transcripts (based on their $P_{adj}$ levels) in the BICC1 KO cells (**m**). For each gene, the normalized expression levels from each of the 6 samples (2 wildtype, KO and 240P each) is shown. (**n**) GSEA plot showing the enrichment of the Hallmark Epithelial_Mesenchymal_Transition data set in the BICC1 KO cells vs. the BICC1 S240P cells.*